Learning to Solve Integer Linear Programs with Davis-Yin Splitting

Anonymous authors
Paper under double-blind review

Abstract

In many applications, a combinatorial problem must be repeatedly solved with similar, but distinct parameters. Yet, the parameters w are not directly observed; only contextual data d that correlates with w is available. It is tempting to use a neural network to predict w given d. However, training such a model requires reconciling the discrete nature of combinatorial optimization with the gradient-based frameworks used to train neural networks. When the problem in question is an Integer Linear Program (ILP), one approach to overcome this training issue is to consider a continuous relaxation of the combinatorial problem. While existing methods utilizing this approach have shown to be highly effective on small problems, they do not always scale well to large problems. In this work, we draw on ideas from modern convex optimization to design a network and training scheme which scales effortlessly to problems with thousands of variables. Our experiments verify the computational advantage our proposed method enjoys on two representative problems, namely the shortest path problem and the knapsack problem.

1 Introduction

Many high-stakes decision problems in healthcare (Zhong & Tang, 2021), logistics and scheduling (Sbihi & Eglese, 2010; Kacem et al., 2021), and transportation (Wang & Tang, 2021) can be viewed as a two step process. In the first step, one gathers data about the situation at hand. This data is used to assign a value (or cost) to outcomes arising from each possible action. The second step is to select the action yielding maximum value (alternatively, lowest cost). Mathematically, this can be framed as an optimization problem with a data-dependent cost function:

$$x^\star(d) \triangleq \operatorname*{arg\,min}_{x \in \mathcal{X}} f(x; d). \tag{1}$$

In this work, we focus on the case where $\mathcal{X} \subset \mathbb{R}^n$ is a finite constraint set and $f(x; d) = w(d)^\top x$ is a linear function. This class of problems is quite rich, containing the shortest path, traveling salesperson, and sequence alignment problems, to name a few. Given $w(d)$, solving equation 1 may be straightforward (*e.g.* shortest path) or NP-hard (*e.g.* traveling salesperson problem (Karp, 1972)). However, our present interest is settings where the dependence of $w(d)$ on d is *unknown*. In such settings, it is intuitive to *learn a mapping* $w_\Theta(d) \approx w(d)$ and then solve

$$x_\Theta(d) \triangleq \operatorname*{arg\,min}_{x \in \mathcal{X}} w_\Theta(d)^\top x \tag{2}$$

in lieu of $w(d)$. The observed data d is called the *context*. As an illustrative running example, consider the shortest path prediction problem shown in Figure 1, which is studied in Berthet et al. (2020) and Pogančić et al. (2019).

At first glance, it may appear natural to tune the weights Θ so as to minimize the difference between $w_\Theta(d)$ and $w(d)$. However, this is only possible if $w(d)$ is available at training time. Even if this approach is feasible, it may not be advisable. If $w_\Theta(d)$ is a near-perfect predictor of $w(d)$ we can expect $x_\Theta(d) \approx x^\star(d)$. However, if there are even small differences between $w_\Theta(d)$ and $w(d)$ this can manifest in wildly different solutions (Bengio, 1997; Wilder et al., 2019). Thus, we focus on methods where Θ is tuned by minimizing the discrepancy between $x_\Theta(d)$ and $x^\star(d)$.

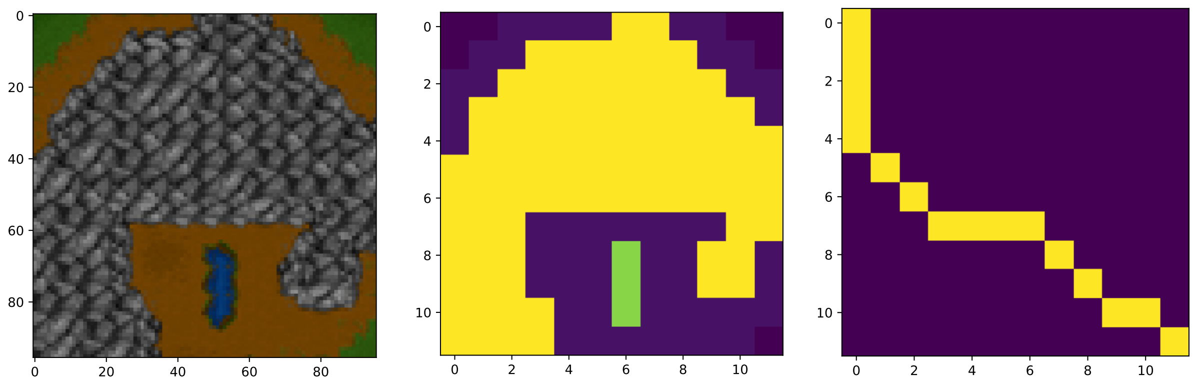

Figure 1: The shortest path prediction problem (Pogančić et al., 2019). The goal is to find the shortest path (from top-left to bottom-right) through a randomly generated terrain map from the Warcraft II tileset (Guyomarch). The contextual data d, shown in (a), is an image sub-divided into 8-by-8 squares, each representing a vertex in a 12-by-12 grid graph. The cost of traversing each square, *i.e.* $w(d)$, is shown in (b), with darker shading representing lower cost. The true shortest path is shown in (c).

The key obstacle in using gradient-based algorithms to tune Θ in such approaches is "differentiating through" the solution $x_\Theta(d)$ of equation 2 to obtain a gradient with which to update Θ. Specifically, the combinatorial nature of $\mathcal{X}$ may cause the solution $x_\Theta(d)$ to remain unchanged for many small perturbations to Θ; yet, for some perturbations $x_\Theta(d)$ may "jump" to a different point in $\mathcal{X}$. Hence, the gradient $\mathrm{d}x_\Theta/\mathrm{d}w_\Theta$ is always either zero or undefined. To compute an informative gradient, we follow Wilder et al. (2019) by relaxing equation 2 to a quadratic program over the convex hull of $\mathcal{X}$ with an added regularizer (see equation 8).

Contribution Drawing upon recent advances in convex optimization (Ryu & Yin, 2022) and implicit neural networks (Fung et al., 2022; McKenzie et al., 2021), we propose a method designed specifically for "differentiating through" large-scale integer linear programs. Our approach is fast, easy to implement using our provided code, and, unlike several prior works (*e.g.* see Pogančić et al. (2019); Berthet et al. (2020)), trains completely on GPU. Numerical examples herein demonstrate our approach, run using only standard computing resources, easily scales to problems with tens of thousands of variables. Theoretically, we verify our approach computes an informative gradient via a refined analysis of Jacobian-free Backpropagation (JFB) (Fung et al., 2022). In summary, we do the following.

- ▷ Building upon McKenzie et al. (2021), we use the three operator splitting technique of Davis & Yin (2017) to propose `DYS-Net`.
- ▷ We provide theoretical guarantees for differentiating through the fixed point of a certain non-expansive, but not contractive, operator.
- ▷ We numerically show `DYS-Net` easily handles combinatorial problems with tens of thousands of variables.

2 Preliminaries

LP Reformulation We focus on optimization problems of the form equation 1 where $f(x;d) = w(d)^\top x$ and $\mathcal{X}$ is the integer or binary points of a polytope, which we may assume to be expressed in standard form (Ziegler, 2012):

$$\mathcal{X} = \mathcal{C} \cap \mathbb{Z}^n \quad \text{or} \quad \mathcal{X} = \mathcal{C} \cap \{0,1\}^n, \quad \text{where} \quad \mathcal{C} = \{x \in \mathbb{R}^n : \; Ax = b \text{ and } x \geq 0\}\,. \tag{3}$$

In other words, equation 1 is an Integer Linear Program (ILP). Similar to works by Elmachtoub & Grigas (2022); Wilder et al. (2019); Mandi & Guns (2020) and others we replace the model equation 2 with its continuous relaxation, and redefine

$$x_\Theta(d) \triangleq \arg\min_{x\in\mathcal{C}} w_\Theta(d)^\top x \tag{4}$$

as a step towards making the computation of $\mathrm{d}x_\Theta/\mathrm{d}w_\Theta$ feasible.

Losses and Training Data We assume access to training data in the tuple form $(d, x^\star(d))$. We focus on the ℓ_2 loss:

$$\mathcal{L}(\Theta) \triangleq \mathbb{E}_{d\sim\mathcal{D}}\left[\ell_2(\Theta; d)\right], \quad \text{where} \quad \ell_2(\Theta; d) = \|x^\star(d) - x_\Theta(d)\|^2, \tag{5}$$

and $\mathcal{D}$ is the distribution of contextual data, although more sophisticated losses can be used with only superficial changes to our results. In principle we select the optimal weights by solving $\arg\min_\Theta \mathcal{L}(\Theta)$. In practice, the population risk is inaccessible, and so we minimize empirical risk instead (Vapnik, 1999):

$$\arg\min_\Theta \frac{1}{N}\sum_{i=1}^{N} \ell_2\left(\Theta; d_i\right). \tag{6}$$

Argmin Differentiation For notational brevity, we temporarily suppress the dependence on d. The gradient of ℓ_2 with respect to Θ, evaluated on a single data point is

$$\frac{\mathrm{d}}{\mathrm{d}\Theta}\left[\ell_2(\Theta)\right] = \frac{\mathrm{d}}{\mathrm{d}\Theta}\left[\|x_\Theta - x^\star\|^2\right] = (x_\Theta - x^\star)^\top \frac{\partial x_\Theta}{\partial w_\Theta}\frac{\mathrm{d}w_\Theta}{\mathrm{d}\Theta}.$$

As discussed in Section 1, $x^\star_\Theta$ is piecewise constant as a function of w_Θ, and this remains true for the LP relaxation equation 4. Consequently, for all w_Θ, either $\partial x_\Theta/\partial\Theta = 0$ or $\partial x_\Theta/\partial\Theta$ is undefined—neither case yields an informative gradient. To remedy this, Wilder et al. (2019); Mandi & Guns (2020) propose adding a small amount of regularization to the objective function in equation 4 to make it strongly convex. This ensures x_Θ is a continuously differentiable function of w_Θ. We add a small quadratic regularizer, modulated by $\gamma \geq 0$, to obtain the objective

$$f_\Theta(x; \gamma, d) \triangleq w_\Theta(d)^\top x + \gamma\|x\|_2^2 \tag{7}$$

and henceforth replace equation 4 by

$$x_\Theta(d) \triangleq \arg\min_{x\in\mathcal{C}} f_\Theta(x; \gamma, d). \tag{8}$$

During training, we aim to solve equation 8 *and* efficiently compute the derivative $\partial x_\Theta/\partial\Theta$.

3 Related Works

We highlight recent works combining optimization—particularly mixed integer programs—and deep learning.

Optimization Layers Introduced in Amos & Kolter (2017), and studied further in Agrawal et al. (2019b;c); Bolte et al. (2021); Blondel et al. (2022), an *optimization layer* is a modular component of a deep learning framework where forward propagation consists of solving a parametrized optimization problem. Consequently, backpropagation entails differentiating the solution to this problem with respect to the parameters. Optimization layers are a promising technology as they are able to incorporate hard constraints into deep neural networks. Moreover, as their output is a (constrained) minimizer of the objective function, it is easier to interpret than the output of a generic layer.

Deep Equilibrium Models Bai et al. (2019); El Ghaoui et al. (2021) propose the notion of *deep equilibrium model* (DEQ), also known as an *implicit neural network*. A DEQ is a neural network for which forward propagation consists of (approximately) computing a fixed point of a parametrized operator. We note that equation 8 may be reformulated as a fixed point problem,

$$\text{Find } x_\Theta \text{ such that } x_\Theta = P_\mathcal{C}\left(x_\Theta - \alpha\nabla_x f_\Theta(x_\Theta; d)\right), \tag{9}$$

where $P_{\mathcal{C}}$ is the orthogonal projection[1] onto $\mathcal{C}$. Thus, DEQ techniques may be applied to constrained optimization layers (Chen et al., 2021; Blondel et al., 2022; McKenzie et al., 2021). However, the cost of computing $P_{\mathcal{C}}$ can be prohibitive, see the discussion in Section 4.

Differentiable Combinatorial Optimizers We now narrow our focus to optimization layers for (integer) linear programs. Wilder et al. (2019) and Elmachtoub & Grigas (2022) are two of the earliest works applying deep learning techniques to data-driven LPs, and delineate two fundamentally different approaches. Specifically, Wilder et al. (2019) proposes replacing the LP with a continuous and strongly convex relaxation, as described in Section 2. This approach is extended to ILPs in Ferber et al. (2020), and to non-quadratic regularizers in Mandi & Guns (2020). On the other hand, Elmachtoub & Grigas (2022) avoid modifying the underlying optimization problem and instead propose a new loss function; dubbed the Smart Predict-then-Optimize (SPO) loss, to be used instead of the ℓ_2 loss. We emphasize that the SPO loss requires access to the true cost vectors $w(d)$, a setting which we do not consider.
Several works define a continuously differentiable proxy for the solution to the *unregularized* LP equation 4, which we rewrite here as[2]

$$x^\star(w) = \operatorname*{arg\,min}_{x\in\mathcal{C}} w^\top x, \tag{10}$$

In Berthet et al. (2020), a stochastic perturbation is considered:

$$x^\star_\varepsilon(w) = \mathbb{E}_Z\left[\operatorname*{arg\,min}_{x\in\mathcal{C}} (w+\varepsilon Z)^\top x\right], \tag{11}$$

which is somewhat analogous to Nesterov-Spokoiny smoothing (Nesterov & Spokoiny, 2017) in zeroth-order optimization. Pogančić et al. (2019) define a piecewise-affine interpolant to $\ell(x^\star(w))$, where ℓ is a suitable loss function.
We note a bifurcation in the literature; Wilder et al. (2019); Ferber et al. (2020); Elmachtoub & Grigas (2022) assume access to training data of the form $(d, w(d))$, whereas Pogančić et al. (2019); Berthet et al. (2020); Sahoo et al. (2022) use training data of the form $(d, x^\star(d))$. Our focus is on the latter setting, and we refer the reader to Kotary et al. (2021) for a recent survey of this area.

Learning-to-Optimize (L2O) Our work can be situated within the broader learning-to-optimize (L2O) framework (Chen et al., 2022; Li & Malik, 2017; Chen et al., 2018; Liu et al., 2023), where an optimization algorithm is learned and its outputs are used to perform inferences. However, traditional L2O methods use a fixed number of layers (*i.e.* unrolled algorithms). Our approach attempts to differentiate through the solution $x^\star_\Theta$ and is therefore most closely aligned with works that employ implicit networks within the L2O framework (Amos & Kolter, 2017; Heaton & Fung, 2023; McKenzie et al., 2021; Gilton et al., 2021; Liu et al., 2022). We highlight that, unlike many L20 works, our goal is not to learn a faster optimization method for fully specified problems. Rather, we seek to solve partially specified problems given contextual data by combining learning and optimization techniques.

Computing the derivative of a minimizer with respect to parameters In all of the aforementioned works, the same fundamental problem is encountered: $\partial x_\Theta/\partial\Theta$ must be computed where x_Θ is the solution of a (constrained) optimization problem with objective function parametrized by Θ. The most common approach to doing so, proposed in Amos & Kolter (2017) and used in Ruthotto et al. (2018); Wilder et al. (2019); Mandi & Guns (2020); Ferber et al. (2020), starts with the KKT conditions for constrained optimality:

$$\frac{\partial f_\Theta}{\partial x}(x_\Theta) + A^\top\hat{\lambda} + \hat{\nu} = 0,\ \ Ax - b = 0,\ \ D(\hat{\nu})x_\Theta = 0,$$

where $\hat{\lambda}$ and $\hat{\nu} \geq 0$ are Lagrange multipliers associated to the optimal solution x_Θ (Bertsekas, 1997) and $D(\hat{\nu})$ is a matrix with $\hat{\nu}$ along its diagonal. Differentiating these equations with respect to Θ and rearranging

[1]For a set $\mathcal{A} \subseteq \mathbb{R}^n$, $P_{\mathcal{A}}(x) \triangleq \operatorname{arg\,min}_{z\in\mathcal{A}} \|z - x\|$.
[2]For sake of notational simplicity, the dependence on d is implicit.

yields

$$\begin{bmatrix} \frac{\partial^2 f_\Theta}{\partial x^2} & A & I \\ A^\top & 0 & 0 \\ D(\hat{\nu}) & 0 & D(x_\Theta) \end{bmatrix} \begin{bmatrix} \frac{dx_\Theta}{d\Theta} \\ \frac{d\hat{\lambda}}{d\Theta} \\ \frac{d\hat{\nu}}{d\Theta} \end{bmatrix} = \begin{bmatrix} \frac{\partial^2 f_\Theta}{\partial x \partial \Theta} \\ 0 \\ 0 \end{bmatrix}. \tag{12}$$

The matrix and right hand side vector in equation 12 are computable, thus enabling one to solve for $\frac{dx_\Theta}{d\Theta}$ (as well as $\frac{d\hat{\lambda}}{d\Theta}$ and $\frac{d\hat{\nu}}{d\Theta}$). The computational bottleneck in this approach is computing the Lagrange multipliers at optimality—*i.e.* $\hat{\lambda}$ and $\hat{\nu}$—in addition to x_Θ. If $x \in \mathbb{R}^n$ and $A \in \mathbb{R}^{m\times n}$ this can be done with a primal-dual interior point method at a cost of $\mathcal{O}\left(\max\{n, m\}^3\right)$ (Amos & Kolter, 2017).
Using the stochastic proxy equation 11, Berthet et al. (2020) derive a formula for $dx^\star_\varepsilon/dw$ which is also an expectation, and hence can be efficiently approximated using Monte Carlo methods. Pogančić et al. (2019) show that the gradients of their interpolant are strikingly easy to compute, requiring just one additional solve of equation 10 with perturbed cost w'. This approach is extended by Sahoo et al. (2022) which proposes to avoid computing $dx^\star_\varepsilon/dw$ entirely, replacing it with the negative identity matrix. This is similar in spirit to our use of Jacobian-free Backpropagation (see Section 4).

4 DYS-Net

We now introduce our proposed model, `DYS-net`. We use this term to refer to the model *and* the training procedure. Fixing an architecture for w_Θ, and an input d, `DYS-net` computes an approximation to $x_\Theta(d)$ in a way that is easy to backpropagate through:

$$\texttt{DYS-net}(d;\ \Theta) \approx x_\Theta \triangleq \operatorname*{arg\,min}_{x\in\mathcal{C}} f_\Theta(x; \gamma, d). \tag{13}$$

The Forward Pass As we wish to compute x_Θ and $\partial x_\Theta/\partial\Theta$ for high dimensional settings (*i.e.* large n), we eschew second-order methods (*e.g.* Newton's method) in favor of first-order methods such as projected gradient descent (PGD). With PGD, a sequence $\{x^k\}$ of estimates of x_Θ are computed so that $x_\Theta = \lim_{k\to\infty} x^k$ where

$$x^{k+1} = P_\mathcal{C}\left(x^k - \alpha\nabla_x f(x^k; \gamma, d)\right) \quad \text{for all } k \in \mathbb{N}.$$

This approach works for simple sets $\mathcal{C}$ for which there exists an explicit form of $P_\mathcal{C}$, *e.g.* when $\mathcal{C}$ is the probability simplex (Duchi et al., 2008; Condat, 2016; Li et al., 2023). However, for general polytopes $\mathcal{C}$ no such form exists, thereby requiring a second iterative procedure, *run at each iteration* k, to compute $P_\mathcal{C}(x^k)$. To avoid this computational expense, we draw on recent advances in the convex optimization literature[3], particularly Davis-Yin splitting or DYS (Davis & Yin, 2017). Specifically, we adapt the architecture incorporating DYS proposed in McKenzie et al. (2021). To this end, we rewrite $\mathcal{C}$ as

$$\mathcal{C} = \{x:\ Ax = b \text{ and } x \geq 0\} = \underbrace{\{x:\ Ax = b\}}_{\triangleq\mathcal{C}_1} \cap \underbrace{\{x:\ x \geq 0\}}_{\triangleq\mathcal{C}_2} = \mathcal{C}_1 \cap \mathcal{C}_2. \tag{14}$$

While $P_\mathcal{C}$ is hard to compute, both $P_{\mathcal{C}_1}$ and $P_{\mathcal{C}_2}$ can be computed cheaply via explicit formulas, once a singular value decomposition (SVD) is computed for A. We verify this via the following lemma (included for completeness, as the two results are already known).

Lemma 1. *If $\mathcal{C}_1, \mathcal{C}_2$ are as in equation 14 and A is full-rank then:*

1. *$P_{\mathcal{C}_1}(z) = z - A^\dagger(Az - b)$, where $A^\dagger = V\Sigma^{-1}U^\top$ and $U\Sigma V^\top$ is the compact SVD of A.*
2. *$P_{\mathcal{C}_2}(z) = \mathrm{ReLU}(z) \triangleq \max\{0, z\}$.*

The following theorem allows one to approximate x_Θ using only $P_{\mathcal{C}_1}$ and $P_{\mathcal{C}_2}$, not $P_\mathcal{C}$.

[3]See Pedregosa & Gidel (2018); Yurtsever et al. (2021) for similar applications of DYS

Theorem 2. *Let $\mathcal{C}_1, \mathcal{C}_2$ be as in equation 14, and suppose $f_\Theta(x;\gamma,d) = w_\Theta(d)^\top x + \frac{\gamma}{2}\|x\|_2^2$ for any neural network $w_\Theta(d)$. For any $\alpha \in (0, 2/\gamma)$ define the sequence $\{z^k\}$ by:*

$$z^{k+1} = T_\Theta(z^k) \quad \textit{for all } k \in \mathbb{N} \tag{15}$$

where

$$T_\Theta(z) \triangleq z - P_{\mathcal{C}_2}(z) + P_{\mathcal{C}_1}\left((2-\alpha\gamma)\, P_{\mathcal{C}_2}(z) - z - \alpha w_\Theta(d)\right). \tag{16}$$

If $x^k \triangleq P_{\mathcal{C}_2}(z^k)$ then $\|x^{k+1} - x^k\|_2^2 = O(1/k)$.

A full proof is included in Appendix A; here we provide a proof sketch. Substituting the gradient

$$\nabla_z f_\Theta(z;\gamma,d) = w_\Theta(d) + \gamma z$$

for $F_\Theta(\cdot, d)$ into the formula for $T_\Theta(\cdot)$ given in McKenzie et al. (2021, Theorem 3.2) and rearranging yields equation 16. Verifying the assumptions of McKenzie et al. (2021, Theorem 3.3) are satisfied is straightforward. For example, $\nabla_z f_\Theta(z;\gamma,d)$ is $1/\gamma$-cocoercive by the Baillon-Haddad theorem (Baillon & Haddad, 1977; Bauschke & Combettes, 2009).
The forward pass of `DYS-net` consists of iterating equation 15 until a suitable stopping criterion is met, which for simplicity we assume to be a maximum number of iterations.

The Backward Pass From Theorem 2 we deduce the following fixed point condition:

$$x_\Theta = P_{\mathcal{C}_2}(z_\Theta), \quad \text{for some} \quad z_\Theta \in \{z : z = T_\Theta(z)\}. \tag{17}$$

As discussed in McKenzie et al. (2021), instead of backpropagating through every iterate of the forward pass, we may derive a formula for $dx_\Theta/d\Theta$ by appealing to the implicit function theorem and differentiating both sides of equation 17:

$$\frac{\mathrm{d}z_\Theta}{\mathrm{d}\Theta} = \frac{\partial T_\Theta}{\partial \Theta} + \frac{\partial T_\Theta}{\partial z}\frac{\mathrm{d}z_\Theta}{\mathrm{d}\Theta} \quad \Longrightarrow \quad \mathcal{J}_\Theta(z_\Theta)\,\frac{\mathrm{d}z_\Theta}{\mathrm{d}\Theta} = \frac{\partial T_\Theta}{\partial \Theta} \text{ where } \mathcal{J}_\Theta(z) = I - \frac{\partial T_\Theta}{\partial z}. \tag{18}$$

We notice two immediate problems not addressed by McKenzie et al. (2021): (i) T_Θ is not everywhere differentiable with respect to z, as $P_{\mathcal{C}_2}$ is not; (ii) if T_Θ were a contraction (*i.e.* Lipschitz in z with constant less than 1), then $\mathcal{J}_\Theta$ would be invertible. However, this is not necessarily the case. Thus, it is not clear *a priori* that equation 18 can be solved for $\mathrm{d}z_\Theta/\mathrm{d}\Theta$. Our key result (Theorem 6 below) is to provide reasonable conditions under which $\mathcal{J}_\Theta(z_\Theta)$ is invertible.

Assuming these issues can be resolved, one may compute the gradient of the loss using the chain rule:

$$\frac{\mathrm{d}\ell}{\mathrm{d}\Theta} = \frac{\mathrm{d}\ell}{\mathrm{d}x}\frac{\mathrm{d}x_\Theta}{\mathrm{d}\Theta} = \frac{\mathrm{d}\ell}{\mathrm{d}x}\left(\frac{\mathrm{d}P_{\mathcal{C}_1}}{\mathrm{d}z}\frac{\mathrm{d}z_\Theta}{\mathrm{d}\Theta}\right) = \frac{\mathrm{d}\ell}{\mathrm{d}x}\frac{\mathrm{d}P_{\mathcal{C}_1}}{\mathrm{d}z}\mathcal{J}_\Theta^{-1}\frac{\partial T_\Theta}{\partial \Theta}$$

This approach requires solving a linear system with $\mathcal{J}_\Theta$ which becomes particularly expensive when n is large. Instead, we use *Jacobian-free Backpropagation* (JFB) (Fung et al., 2022), also known as one-step differentiation (Bolte et al., 2024), in which the Jacobian $\mathcal{J}_\Theta$ is replaced with the identity matrix. This leads to an approximation of the true gradient $\mathrm{d}\ell/\mathrm{d}\Theta$ using

$$p_\Theta(x_\Theta) = \left[\frac{\partial \ell}{\partial x}\frac{\mathrm{d}P_{\mathcal{C}_1}}{\mathrm{d}z}\frac{\partial T_\Theta}{\partial \Theta}\right]_{(x,z)=(x_\Theta,z_\Theta)}. \tag{19}$$

We show equation 19 is a valid descent direction by resolving the two problems highlighted above. We begin by rigorously deriving a formula for $\partial T_\Theta/\partial z$. Recall the following generalization of the Jacobian to non-smooth operators due to Clarke (1983).

Definition 3. *For any locally Lipshitz $F : \mathbb{R}^n \to \mathbb{R}^n$ let D_F denote the set upon which F is differentiable. The Clarke Jacobian of F is the set-valued function defined as*

$$\partial F(\bar{z}) = \begin{cases} \left.\frac{\mathrm{d}F}{\mathrm{d}z}\right|_{z=\bar{z}} & \textit{if } \bar{z} \in D_F \\ \mathrm{Con}\left\{\lim_{z' \to \bar{z}: z' \in D_F} \left.\frac{\mathrm{d}F}{\mathrm{d}z}\right|_{z=z'}\right\} & \textit{if } \bar{z} \notin D_F \end{cases}$$

Where Con {} *denotes the convex hull of a set.*

Algorithm 1 `DYS-Net`

```
1: Inputs: $A$ and $b$ defining $\mathcal{C}$, hyperparameters $\alpha, \gamma, K$
2: Initialize: Attach neural network $w_\Theta(\cdot)$. Compute SVD of $A$ for $P_{\mathcal{C}_1}$ formula
3: Forward Pass: Initialize $z^0$. Given $w_\Theta(d)$ compute $z^1, \ldots, z^K$ using equation 15. Return $x^K \triangleq P_{\mathcal{C}_1}(z^K) \approx x_\Theta$.
4: Backward Pass: Compute $p_\Theta(x^K) \approx p_\Theta(x_\Theta)$ using equation 19 and return.
```

The Clarke Jacobian of $P_{\mathcal{C}_2}$ is easily computable, see Lemma 9. Define the (set-valued) functions

$$c(\alpha) \triangleq \partial \max(0, \alpha) = \begin{cases} 1 & \text{if } \alpha > 0 \\ 0 & \text{if } \alpha < 0 \\ [0,1] & \text{if } \alpha = 0 \end{cases} \quad \text{and} \quad \tilde{c}(\alpha) = \begin{cases} 1 & \text{if } \alpha > 0 \\ 0 & \text{if } \alpha \leq 0 \end{cases}$$

Then

$$\partial P_{\mathcal{C}_2}(\bar{z}) = \left[\frac{\mathrm{d}}{\mathrm{d}z}\operatorname{ReLU}(z)\right]_{z=\bar{z}} = \operatorname{diag}(c(\bar{z})), \tag{20}$$

where c is applied element-wise. We shall now provide a consistent rule for selecting, at any $\bar{z}$, an element of $\partial P_{\mathcal{C}_2}(\bar{z})$. If $z_i \neq 0$ for all i then $\partial P_{\mathcal{C}_2}$ is a singleton. If one or more $z_i = 0$ then $\partial P_{\mathcal{C}_2}$ is multi-valued, so we choose the element of $\partial P_{\mathcal{C}_2}$ with 0 in the (i,i) position for every $z_i = 0$. We write $dP_{\mathcal{C}_2}/dz$ for this chosen element, and note that

$$\left.\frac{\mathrm{d}P_{\mathcal{C}_2}}{\mathrm{d}z}\right|_{z=\bar{z}} = \operatorname{diag}(\tilde{c}(\bar{z})) \in \partial P_{\mathcal{C}_2}(\bar{z})$$

This aligns with the default rule for assigning a sub-gradient to ReLU used in the popular machine learning libraries TensorFlow(Abadi et al., 2016), PyTorch (Paszke et al., 2019) and JAX (Bradbury et al., 2018), and has been observed to yield networks which are more stable to train than other choices (Bertoin et al., 2021).

Given the above convention, we can compute $\partial T_\Theta/\partial z$, interpreted as an element of the Clarke Jacobian of T_Θ chosen according to a consistent rule. Surprisingly, $\partial T_\Theta/\partial z$ may be expressed using only orthogonal projections to hyperplanes. Throughout, we let $e_i \in \mathbb{R}^n$ be the one-hot vector with 1 in the i-th position and zeros elsewhere, and $a_i^\top$ be the i-th row of A. For any subspace $\mathcal{H}$ we denote the orthogonal subspace as $\mathcal{H}^\perp$. The following theorem, the proof of which is given in Appendix A, characterizes $\partial T_\Theta/\partial z$.

Theorem 4. *Suppose A is full-rank and $\mathcal{H}_1 \triangleq \operatorname{Null}(A)$, $\mathcal{H}_{2,z} \triangleq \operatorname{Span}(e_i : z_i > 0)$. Then for all $\hat{z} \in \mathbb{R}^n$*

$$\left.\frac{\partial T_\Theta}{\partial z}\right|_{z=\bar{z}} = P_{\mathcal{H}_1^\perp} P_{\mathcal{H}_{2,\bar{z}}^\perp} + (1 - \alpha\gamma) \cdot P_{\mathcal{H}_1} P_{\mathcal{H}_{2,\bar{z}}}. \tag{21}$$

To show JFB is applicable, it suffices to verify $\|\partial T_\Theta/\partial z\| < 1$ when evaluated at z_Θ. Theorem 4 enables us to show this inequality holds when x_Θ satisfies a commonly-used regularity condition, which we formalize as follows.

Definition 5 (LICQ condition, specialized to our case)**.** *Let x_Θ denote the solution to equation 8. Let $\mathcal{A}(x_\Theta) \subseteq \{1, \ldots, n\}$ denote the set of active positivity constraints:*

$$\mathcal{A}(x_\Theta) \triangleq \{i : [x_\Theta]_i = 0\}. \tag{22}$$

The point x_Θ satisfies the Linear Independence Constraint Qualification *(LICQ) condition if the vectors*

$$\{a_1, \ldots, a_m\} \cup \{e_i : i \in \mathcal{A}(x_\Theta)\} \tag{23}$$

are linearly independent.

Theorem 6. *If the LICQ condition holds at x_Θ, A is full-rank and $\alpha \in (0, 2/\gamma)$, then $\|\partial T_\Theta/\partial z\|_{z=z_\Theta} < 1$.*

The significance of Theorem 6, which is proved in Appendix A, is outlined by the following corollary, stating that using p_Θ instead of the true gradient $d\ell/d\Theta$ is still guaranteed to decrease $\ell(\Theta)$, at least for small enough step-size.

Corollary 7. *If T_Θ is continuously differentiable with respect to Θ at z_Θ, the assumptions in Theorem 6 hold and $(\partial T_\Theta/\partial\Theta)^\top(\partial T_\Theta/\partial\Theta)$ has condition number sufficiently small, then $p_\Theta(x_\Theta)$ is a descent direction for ℓ with respect to Θ.*

Theorem 6 also proves that $\mathcal{J}_\Theta(z_\Theta)$ in equation 18 is invertible, thus also justifying the use of Jacobian-based backprop as well as numerous other gradient approximation techniques (Liao et al., 2018; Geng et al., 2021).

Finally, we note that in practice $p_\Theta(x^K)$ is used instead of $p_\Theta(x_\Theta)$. Fung et al. (2022, Corollary 0.1) guarantees that $p_\Theta(x^K)$ will still be a descent direction for K sufficiently large, see also Bolte et al. (2024, Cor. 1).

Implementation `DYS-net` is implemented as an abstract PyTorch (Paszke et al., 2019) layer in the provided code. To instantiate it, a user only need specify A and b (see equation 3) and choose an architecture for w_Θ. At test time, it can be beneficial to solve the underlying combinatorial problem equation 2 exactly using a specialized algorithm, *e.g.* commercial integer programming software for the knapsack prediction problem. This can easily be done using `DYS-net` by instantiating the `test-time-forward` abstract method.

5 Numerical Experiments

5.1 Experiments using `PyEPO`

First, we verify the efficiency of `DYS-net` by performing benchmarking experiments within the `PyEPO` (Tang & Khalil, 2022) framework. We compare `DYS-net` against three other methods: Perturbed Optimization (Berthet et al., 2020)—`PertOpt-net`; an approach using Blackbox Backpropagation (Vlastelica et al., 2019)—`BB-net`; and an approach using `cvxpylayers` (Agrawal et al., 2019a)—`CVX-net`.

Models We use the `PyEPO` implementations of Perturbed Optimization, respectively Blackbox Backpropagation, as the core of `PertOpt-net`, respectively `BB-net`. We use the same architecture for $w_\Theta(d)$ for all models[4] and use an appropriate combinatorial solver at test time, via the `PyEPO` interface to `Gurobi`. Thus, the methods differ *only in training procedure*. The precise architectures used for $w_\Theta(d)$ for each problem are described in Appendix C, and are also viewable in the accompanying code repository . Interestingly, we observed that adding drop-out during training to the output layer proved beneficial for the knapsack prediction problem. Without this, we find that w_Θ tends to output a sparse approximation to w supported on a feasible set of items, and so does not generalize well.

Training We train for a maximum of 100 epochs or 30 minutes, whichever comes first. We use a validation set for model selection as we observe that, for all methods, the best loss is seldom achieved at the final iteration. Exact hyperparameters are discussed in the appendix. For each problem size, we perform three repeats with different randomly generated data. Results are displayed in Figure 2.

Evaluation Given test data $\{(d_i, w(d_i), x^\star(d_i))\}_{i=1}^N$ and a fully trained model $w_\Theta(d)$ we define the *regret* as:

$$r(d) = w(d_i)^\top \left(x_\Theta(d_i) - x^\star(d_i)\right). \tag{24}$$

Note that regret is non-negative, and is zero precisely when $x_\Theta(d_i)$ is a solution of equal quality to $x^\star(d_i)$. Following Tang & Khalil (2022), we evaluate the quality of $w_\Theta(d)$ using *normalized regret*, defined as

$$\tilde{r} = \frac{\sum_{i=1}^N r(d_i)}{\sum_{i=1}^N \left[w(d_i)^\top x^\star(d_i)\right]}. \tag{25}$$

[4]The architecture we use for shortest path prediction problems differs from that used for knapsack prediction problems. See the appendix for details.

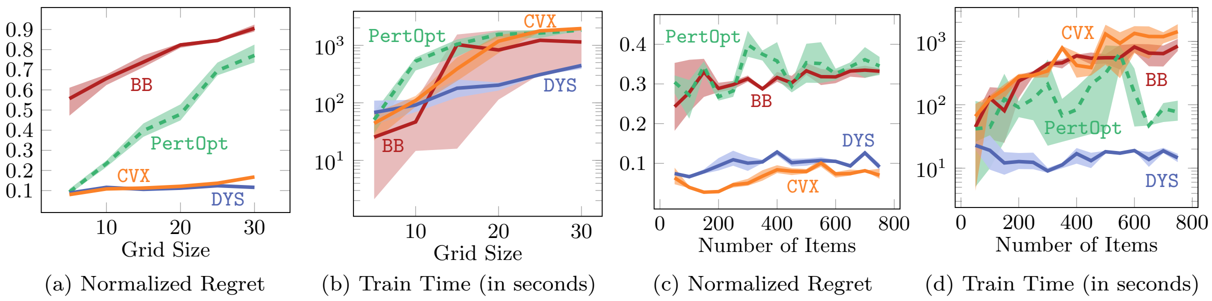

Figure 2: Results for the shortest path and knapsack prediction problems. Figures (a) and (b) show normalized regret and train time for the shortest path prediction problem, while Figures (c) and (d) show normalized regret and train time for the knapsack prediction problem. Note that the train time in figures (b) and (d) is the time till the model achieving best normalized regret on the validation set is reached.

5.1.1 Shortest Path Prediction

The shortest path between two vertices in a graph $\mathcal{G} = (\mathcal{V}, \mathcal{E})$ can be found by:

$$x^\star = \arg\min_{x\in\mathcal{X}} w(d)^\top x;\ \ \mathcal{X} = \{x \in \{0,1\}^{|\mathcal{E}|} : Ex = b\}, \tag{26}$$

where E is the vertex-edge adjacency matrix, b encodes the initial and terminal vertices, and $w(d) \in \mathbb{R}^{|\mathcal{E}|}$ is a vector encoding (d-dependent) edge lengths; see Appendix for further details. Here, $x^\star$ will encode the edges included in the optimal path. In this experiment we focus on the case where $\mathcal{G}$ is the $k \times k$ grid graph. We use the `PyEPO` Tang & Khalil (2022) benchmarking software to generate training datasets of the form $\{(d_i, x_i^\star \approx x^\star(d_i))\}_{i=1}^N$ where $N = 1000$ for each $k \in \{5, 10, 15, 20, 25, 30\}$. The d_i are sampled from the five-dimensional multivariate Gaussian distribution with mean 0 and identity covariance. Note that the number of variables in equation 26 scales like k^2, not k.

5.1.2 Knapsack Prediction

In the (0–1, single) knapsack prediction problem, we are presented with a container (*i.e.* a knapsack) of size c and I items, of sizes $s_1, \dots, s_I$ and values $w_1(d), \dots, w_I(d)$. The goal is to select the subset of maximum value that fits in the container, *i.e.* to solve:

$$x^\star = \arg\max_{x\in\mathcal{X}} w(d)^\top x;\ \ \mathcal{X} = \{x \in \{0,1\}^I :\ s^\top x \le c\}$$

Here, $x^\star$ encodes the selected items. In the (0–1) k-knapsack prediction problem we imagine the container having various notions of "size" (i.e. length, volume, weight limit) and hence a k-tuple of capacities $c \in \mathbb{R}^k$. Correspondingly, the items each have a k-tuple of sizes $s_1, \dots, s_I \in \mathbb{R}^k$. We aim to select a subset of maximum value, amongst all subsets satisfying the k capacity constraints:

$$\begin{aligned} x^\star &= \arg\max_{x\in\mathcal{X}} w(d)^\top x \\ \mathcal{X} &= \{x \in \{0,1\}^I :\ Sx \le c\} \\ S &= \begin{bmatrix} s_1 & \cdots & s_k \end{bmatrix} \in \mathbb{R}^{k\times I} \end{aligned} \tag{27}$$

In Appendix B we discuss how to transform $\mathcal{X}$ into the canonical form discussed in Section 2. We again use `PyEPO` to generate datasets of the form $\{(d_i, x_i^\star \approx x^\star(d_i))\}_{i=1}^N$ where $N = 1000$ for $k = 2$ and I varying from 50 to 750 inclusive in increments of 50. The d_i from the five-dimensional multivariate Gaussian distribution with mean 0 and identity covariance.

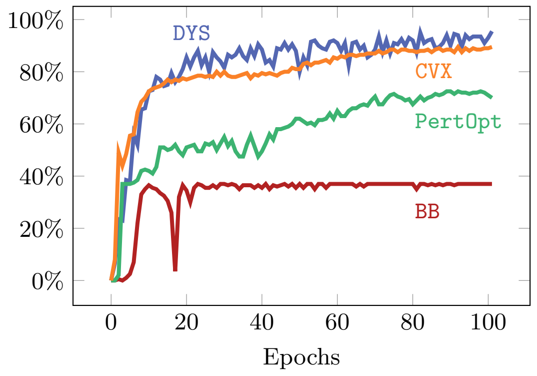

Figure 3: Accuracy (in percentage) of predicted paths on 5-by-5 grid during training.

grid size	number of variables	network size
5-by-5	40	500
10-by-10	180	2040
20-by-20	760	8420
30-by-30	1740	19200
50-by-50	4900	53960
100-by-100	19800	217860

Table 1: Number of variables (*i.e.* number of edges) per grid size for the shortest path prediction problem of Section 5.2. Third column: number of parameters in $w_\Theta(d)$ for `DYS-Net`, `CVX-net` and `PertOpt-net`. For `BB-Net`, we found a latent dimension that is 20-times larger than the aforementioned three to be more effective.

5.1.3 Results

As is clear from Figure 2 `DYS-net` trains the fastest among the four methods, and achieves the best or near-best normalized regret in all cases.

5.2 Large-scale shortest path prediction

Our shortest path prediction experiment described in Section 5.1.1 is bottlenecked by the fact that the "academic" license of `Gurobi` does not allow for shortest path prediction problems on grids larger than 30×30. To further explore the limits of `DYS-net`, we redo this experiment using a custom `pyTorch` implementation of Dijkstra's algorithm[5] as our base solver for equation 26.

Data Generation We generate datasets $\mathcal{D} = \{(d_i, x^\star(d_i))\}_{i=1}^{1,000}$ for k-by-k grids where $k \in \{5, 10, 20, 30, 50, 100\}$ and the d_i are sampled uniformly at random from $[0,1]^5$, the true edge weights are computed as $w(d) = Wd$ for fixed $W \in \mathbb{R}^{|\mathcal{E}|\times 5}$, and $x^\star(d)$ is computed given $w(d)$ using the aforementioned `pyTorch` implementation of Dijkstra's algorithm. Further details are presented in Appendix C.

Models and Training We test the same four approaches as in Sections 5.1.1 and 5.1.2, but unlike in these sections we do not use the `PyEPO` implementations of `PertOpt-net` or `BB-net`. We cannot, as the `PyEPO` implementations call `Gurobi` to solve equation 26 which, as mentioned above, cannot handle grids larger than 30×30. Instead, we use custom implementations based on the code accompanying the works introducing `PertOpt` (Berthet et al., 2020) and `BB` (Vlastelica et al., 2019). We use the same architecture for $w_\Theta(d)$ for `DYS-net`, `PertOpt-net`, and `Cvx-net`; a two layer fully connected neural network with leaky

[5]adapted from `Tensorflow` code available at `https://github.com/google-research/google-research/blob/master/perturbations/experiments/shortest_path.py`

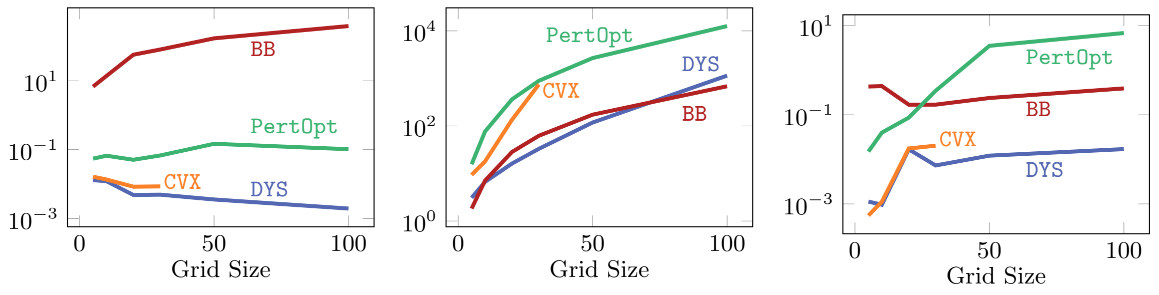

(a) Test MSE Loss (b) Training Time (min) (c) Regret Values

Figure 4: Results for the shortest path prediction problem. a) Test MSE loss (left), b) training time in minutes (middle), and c) regret values (right) vs. gridsize for DYS-Net (proposed) and approaches using `cvxpylayers` (Agrawal et al., 2019b) labeled CVX; Perturbed Optimization (Berthet et al., 2020) labeled PertOpt; and Blackbox Backpropagation (Vlastelica et al., 2019), labeled BB. Note CVX is unable to load or run problems with gridsize over 30. Dimensions of the variables can be found in Table 1.

ReLU activation functions. For `DYS-net` and `Cvx-net` we *do not* modify the forward pass at test time. For `BB-net` we use a larger network by making the latent dimension 20-times larger than that of the first three as we found this more effective. Network sizes can be seen in Table 1.
We tuned the hyperparameters for each approach to the best of our ability on the smallest problem (5-by-5 grid) and then used these hyperparameter values for all other graph sizes. See Figure 3 for the results of this training run. We train all approaches for 100 epochs total on each problem using the ℓ_2 loss equation 5.

Results The results are displayed in Figure 4. While `CVX-net` and `PertOpt-net` achieve low regret for small grids, `DYS-net` model achieves a low regret *for all* grids. In addition to training faster, `DYS-net` can also be trained for much larger problems, *e.g.*, 100-by-100 grids, as shown in Figure 4. We found that `CVX-net` could not handle grids larger than 30-by-30, *i.e.* , problems with more than 1740 variables[6] (see Table 1). Importantly, `PertOpt-net` takes close to a week to train for the 100-by-100 problem, whereas `DYS-net` takes about a day (see right Figure 4b). On the other hand, the training speed of `BB-net` is comparable to that of `DYS-net`, but does not lead to competitive accuracy as shown in Figure 4(a). Interpreting the outputs of `DYS-net` and `CVX-net` as (unnormalized) probabilities over the grid, one can use a greedy algorithm to determine the most probable path from top-left to bottom-right. For small grids, *e.g.* 5-by-5, this path coincides exactly with the true path for most d (see Fig. 3).

5.3 Warcraft shortest path prediction

Finally, as an illustrative example, we consider the Warcraft terrains dataset first studied in Vlastelica et al. (2019). As shown in Figure 1, d is a 96-by-96 RGB image, divided into a 12-by-12 grid of terrain tiles. Each tile has a different cost to traverse, and the goal is to find the quickest path from the top-left corner to the bottom-right corner.

Models, Training, and Evaluation We build upon the code provided as part of the `PyEPO` package (Tang & Khalil, 2022). We use the same architecture for $w_\Theta(d)$ for `BB-net`, `PertOpt-net`, and `DYS-net`—a truncated ResNet18 (He et al., 2016) as first proposed in Vlastelica et al. (2019). The baseline is the same truncated ResNet18 architecture trained to predict $x^\star(d)$ *directly*. We train each network for 50 epochs, except for the baseline, which is trained for 150 epochs. The initial learning rate is 5×10^{-4} and it is decreased by a factor of 10 after 30 and 40 epochs respectively. `PertOpt-net` and `DYS-net` are trained to minimize the ℓ_2 loss equation 5, while `BB-net` is trained to minimize the Hamming loss as described in Vlastelica et al. (2019). Given test data $\{(d_i, w(d_i), x^\star(d_i))\}_{i=1}^N$, we follow Tang & Khalil (2022) and evaluate

[6]This is to be expected, as discussed in in Amos & Kolter (2017); Agrawal et al. (2019a)

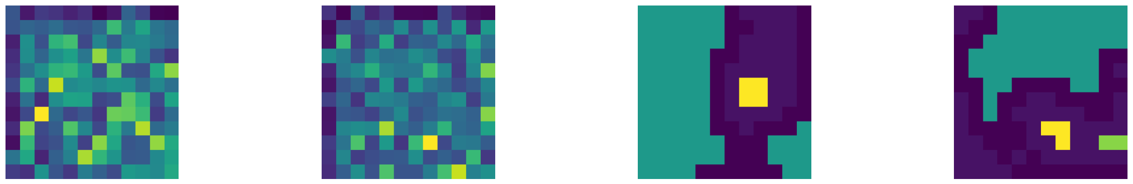

Figure 5: **Left two figures:** Sample cost matrices for shortest problem considered in Section 5.1.1. **Right two figures:** Sample cost matrices for the Warcraft shortest path prediction problem considered in Section 5.3. Note that in Section 5.3 the node weighted shortest path prediction problem is considered, while in Section 5.1.1 the edge weighted variant is solved. For ease of comparison, in the left two figures we have reshaped the edge cost vector into a node cost matrix.

Algorithm	Test Relative Regret	Prediction Accuracy	Time (in hours)
Baseline	19.1150	0.0%	0.07
`BB-net`	0.1435	91.43%	5.56
`PertOpt-net`	0.4566	35.71%	3.15
`DYS-net`	0.2745	51.43%	4.13

Table 2: Results for the 12-by-12 Warcraft shortest path prediction problem. The low relative regret of `BB-net` could be attributed to the "discrete" nature of the true cost vectors as well as its use of the Hamming loss in training.

a fully trained model $w_\Theta(d)$ using *relative regret*:

$$\hat{r} = \sum_{i=1}^{N} \frac{r(d_i)}{w(d_i)^\top x^\star(d_i)} \tag{28}$$

Results The results for this experiment are shown in Table 2. Interestingly, `BB-net` and `PertOpt-net` are much more competitive in this experiment than in the experiements of Sections 5.1.1, 5.1.2, and 5.2. We attribute this to the "discrete" nature of the true cost vector $w(d)$—for the Warcraft problem entries of $w(d)$ can only take on four, well-separated values—as opposed to the more "continuous" nature of $w(d)$ in the previous experiments. This difference is illustrated in Figure 5.

6 Conclusions

This work presents a new method for learning to solve ILPs using Davis-Yin splitting which we call `DYS-net`. We prove that the gradient approximation computed in the backward pass of `DYS-net` is indeed a descent direction, thus advancing the current understanding of implicit networks. Our experiments show that `DYS-net` is capable of scaling to truly large ILPs, and outperforms existing state-of-the-art methods in some settings. Our experiments also reveal an interesting dichotomy between problems in which entries of $w(d)$ may take on only a handful of discrete values and problems in which $w(d)$ is more "continuous". Future work could explore this dichotomy further, as well as apply `DYS-net` to additional ILPs, for example the traveling salesman problem.

References

Martin Abadi, Paul Barham, Jianmin Chen, Zhifeng Chen, Andy Davis, Jeffrey Dean, Matthieu Devin, Sanjay Ghemawat, Geoffrey Irving, Michael Isard, et al. Tensorflow: a system for large-scale machine learning. In *12th USENIX symposium on operating systems design and implementation (OSDI 16)*, pp. 265–283, 2016.

A. Agrawal, B. Amos, S. Barratt, S. Boyd, S. Diamond, and Z. Kolter. Differentiable convex optimization layers. In *Advances in Neural Information Processing Systems*, 2019a.

Akshay Agrawal, Brandon Amos, Shane Barratt, Stephen Boyd, Steven Diamond, and J Zico Kolter. Differentiable convex optimization layers. *Advances in neural information processing systems*, 32, 2019b.

Akshay Agrawal, Shane Barratt, Stephen Boyd, Enzo Busseti, and Walaa M Moursi. Differentiating through a cone program. *arXiv preprint arXiv:1904.09043*, 2019c.

Brandon Amos and J Zico Kolter. Optnet: Differentiable optimization as a layer in neural networks. In *International Conference on Machine Learning*, pp. 136–145. PMLR, 2017.

Shaojie Bai, J Zico Kolter, and Vladlen Koltun. Deep equilibrium models. *Advances in Neural Information Processing Systems*, 32, 2019.

Jean-Bernard Baillon and Georges Haddad. Quelques propriétés des opérateurs angle-bornés et n-cycliquement monotones. *Israel Journal of Mathematics*, 26:137–150, 1977.

Heinz H Bauschke and Patrick L Combettes. The Baillon-Haddad theorem revisited. *arXiv preprint arXiv:0906.0807*, 2009.

Yoshua Bengio. Using a financial training criterion rather than a prediction criterion. *International journal of neural systems*, 8(04):433–443, 1997.

Quentin Berthet, Mathieu Blondel, Olivier Teboul, Marco Cuturi, Jean-Philippe Vert, and Francis Bach. Learning with differentiable perturbed optimizers. *Advances in neural information processing systems*, 33: 9508–9519, 2020.

David Bertoin, Jérôme Bolte, Sébastien Gerchinovitz, and Edouard Pauwels. Numerical influence of ReLU'(0) on backpropagation. *Advances in Neural Information Processing Systems*, 34:468–479, 2021.

Dimitri P Bertsekas. Nonlinear programming. *Journal of the Operational Research Society*, 48(3):334–334, 1997.

Mathieu Blondel, Quentin Berthet, Marco Cuturi, Roy Frostig, Stephan Hoyer, Felipe Llinares-López, Fabian Pedregosa, and Jean-Philippe Vert. Efficient and modular implicit differentiation. *Advances in neural information processing systems*, 35:5230–5242, 2022.

Jérôme Bolte, Tam Le, Edouard Pauwels, and Tony Silveti-Falls. Nonsmooth implicit differentiation for machine-learning and optimization. *Advances in neural information processing systems*, 34:13537–13549, 2021.

Jérôme Bolte, Edouard Pauwels, and Samuel Vaiter. One-step differentiation of iterative algorithms. *Advances in Neural Information Processing Systems*, 36, 2024.

James Bradbury, Roy Frostig, Peter Hawkins, Matthew James Johnson, Chris Leary, Dougal Maclaurin, George Necula, Adam Paszke, Jake VanderPlas, Skye Wanderman-Milne, et al. Jax: composable transformations of python+ numpy programs. 2018.

Bingqing Chen, Priya L Donti, Kyri Baker, J Zico Kolter, and Mario Bergés. Enforcing policy feasibility constraints through differentiable projection for energy optimization. In *Proceedings of the Twelfth ACM International Conference on Future Energy Systems*, pp. 199–210, 2021.

Tianlong Chen, Xiaohan Chen, Wuyang Chen, Howard Heaton, Jialin Liu, Zhangyang Wang, and Wotao Yin. Learning to optimize: A primer and a benchmark. *Journal of Machine Learning Research*, 23(189): 1–59, 2022.

Xiaohan Chen, Jialin Liu, Zhangyang Wang, and Wotao Yin. Theoretical linear convergence of unfolded ista and its practical weights and thresholds. *Advances in Neural Information Processing Systems*, 31, 2018.

FH Clarke. Optimization and nonsmooth analysis, wiley-interscience. *New York*, 1983.

Laurent Condat. Fast projection onto the simplex and the ℓ_1 ball. *Mathematical Programming*, 158(1): 575–585, 2016.

Damek Davis and Wotao Yin. A three-operator splitting scheme and its optimization applications. *Set-valued and variational analysis*, 25(4):829–858, 2017.

John Duchi, Shai Shalev-Shwartz, Yoram Singer, and Tushar Chandra. Efficient projections onto the ℓ_1-ball for learning in high dimensions. In *Proceedings of the 25th international conference on Machine learning*, pp. 272–279, 2008.

Laurent El Ghaoui, Fangda Gu, Bertrand Travacca, Armin Askari, and Alicia Tsai. Implicit deep learning. *SIAM Journal on Mathematics of Data Science*, 3(3):930–958, 2021.

Adam N Elmachtoub and Paul Grigas. Smart "predict, then optimize". *Management Science*, 68(1):9–26, 2022.

Aaron Ferber, Bryan Wilder, Bistra Dilkina, and Milind Tambe. Mipaal: Mixed integer program as a layer. In *Proceedings of the AAAI Conference on Artificial Intelligence*, volume 34, pp. 1504–1511, 2020.

Samy Wu Fung, Howard Heaton, Qiuwei Li, Daniel McKenzie, Stanley Osher, and Wotao Yin. JFB: Jacobian-free backpropagation for implicit networks. In *Proceedings of the AAAI Conference on Artificial Intelligence*, 2022.

Zhengyang Geng, Xin-Yu Zhang, Shaojie Bai, Yisen Wang, and Zhouchen Lin. On training implicit models. *Advances in Neural Information Processing Systems*, 34:24247–24260, 2021.

Davis Gilton, Gregory Ongie, and Rebecca Willett. Deep equilibrium architectures for inverse problems in imaging. *IEEE Transactions on Computational Imaging*, 7:1123–1133, 2021.

Jean Guyomarch. Warcraft ii open-source map editor, 2017. *http://github. com/war2/war2edit*.

Kaiming He, Xiangyu Zhang, Shaoqing Ren, and Jian Sun. Deep residual learning for image recognition. In *Proceedings of the IEEE conference on computer vision and pattern recognition*, pp. 770–778, 2016.

Howard Heaton and Samy Wu Fung. Explainable ai via learning to optimize. *Scientific Reports*, 13(1):10103, 2023.

Imed Kacem, Hans Kellerer, and A Ridha Mahjoub. Preface: New trends on combinatorial optimization for network and logistical applications. *Annals of Operations Research*, 298(1):1–5, 2021.

Richard M Karp. Reducibility among combinatorial problems. In *Complexity of computer computations*, pp. 85–103. Springer, 1972.

James Kotary, Ferdinando Fioretto, Pascal van Hentenryck, and Bryan Wilder. End-to-end constrained optimization learning: A survey. In *30th International Joint Conference on Artificial Intelligence, IJCAI 2021*, pp. 4475–4482. International Joint Conferences on Artificial Intelligence, 2021.

Ke Li and Jitendra Malik. Learning to optimize. In *International Conference on Learning Representations*, 2017.

Qiuwei Li, Daniel McKenzie, and Wotao Yin. From the simplex to the sphere: faster constrained optimization using the hadamard parametrization. *Information and Inference: A Journal of the IMA*, 12(3):1898–1937, 2023.

Renjie Liao, Yuwen Xiong, Ethan Fetaya, Lisa Zhang, KiJung Yoon, Xaq Pitkow, Raquel Urtasun, and Richard Zemel. Reviving and improving recurrent back-propagation. In *International Conference on Machine Learning*, pp. 3082–3091. PMLR, 2018.

Jialin Liu, Xiaohan Chen, Zhangyang Wang, Wotao Yin, and HanQin Cai. Towards constituting mathematical structures for learning to optimize. In *International Conference on Machine Learning*, pp. 21426–21449. PMLR, 2023.

Jiaming Liu, Xiaojian Xu, Weijie Gan, Ulugbek Kamilov, et al. Online deep equilibrium learning for regularization by denoising. *Advances in Neural Information Processing Systems*, 35:25363–25376, 2022.

Jayanta Mandi and Tias Guns. Interior point solving for lp-based prediction+ optimisation. *Advances in Neural Information Processing Systems*, 33:7272–7282, 2020.

Daniel McKenzie, Howard Heaton, Qiuwei Li, Samy Wu Fung, Stanley Osher, and Wotao Yin. Operator splitting for learning to predict equilibria in convex games. *arXiv e-prints*, pp. arXiv–2106, 2021.

Yurii Nesterov and Vladimir Spokoiny. Random gradient-free minimization of convex functions. *Foundations of Computational Mathematics*, 17:527–566, 2017.

Adam Paszke, Sam Gross, Francisco Massa, Adam Lerer, James Bradbury, Gregory Chanan, Trevor Killeen, Zeming Lin, Natalia Gimelshein, Luca Antiga, et al. Pytorch: An imperative style, high-performance deep learning library. *Advances in Neural Information Processing Systems*, 32, 2019.

Fabian Pedregosa and Gauthier Gidel. Adaptive three operator splitting. In *International Conference on Machine Learning*, pp. 4085–4094. PMLR, 2018.

Marin Vlastelica Pogančić, Anselm Paulus, Vit Musil, Georg Martius, and Michal Rolinek. Differentiation of blackbox combinatorial solvers. In *International Conference on Learning Representations*, 2019.

Lars Ruthotto, Julianne Chung, and Matthias Chung. Optimal experimental design for inverse problems with state constraints. *SIAM Journal on Scientific Computing*, 40(4):B1080–B1100, 2018.

Ernest Ryu and Wotao Yin. *Large-Scale Convex Optimization: Algorithm Designs via Monotone Operators*. Cambridge University Press, Cambridge, England, 2022.

Subham Sekhar Sahoo, Anselm Paulus, Marin Vlastelica, Vít Musil, Volodymyr Kuleshov, and Georg Martius. Backpropagation through combinatorial algorithms: Identity with projection works. In *The Eleventh International Conference on Learning Representations*, 2022.

Abdelkader Sbihi and Richard W Eglese. Combinatorial optimization and green logistics. *Annals of Operations Research*, 175(1):159–175, 2010.

Bo Tang and Elias Boutros Khalil. Pyepo: A pytorch-based end-to-end predict-then-optimize library with linear objective function. In *OPT 2022: Optimization for Machine Learning (NeurIPS 2022 Workshop)*, 2022.

Vladimir Vapnik. *The nature of statistical learning theory*. Springer science & business media, 1999.

Marin Vlastelica, Anselm Paulus, Vit Musil, Georg Martius, and Michal Rolinek. Differentiation of blackbox combinatorial solvers. In *International Conference on Learning Representations*, 2019.

Qi Wang and Chunlei Tang. Deep reinforcement learning for transportation network combinatorial optimization: A survey. *Knowledge-Based Systems*, 233:107526, 2021.

Bryan Wilder, Bistra Dilkina, and Milind Tambe. Melding the data-decisions pipeline: Decision-focused learning for combinatorial optimization. In *Proceedings of the AAAI Conference on Artificial Intelligence*, volume 33, pp. 1658–1665, 2019.

Alp Yurtsever, Varun Mangalick, and Suvrit Sra. Three operator splitting with a nonconvex loss function. In *International Conference on Machine Learning*, pp. 12267–12277. PMLR, 2021.

Liwei Zhong and Guochun Tang. Preface: Combinatorial optimization drives the future of health care. *Journal of Combinatorial Optimization*, 42(4):675–676, 2021.

Günter M Ziegler. *Lectures on polytopes*, volume 152. Springer Science & Business Media, 2012.

A Appendix A: Proofs

For the reader's convenience we restate each result given in the main text before proving it.

Theorem 2. *Let $\mathcal{C}_1, \mathcal{C}_2$ be as in equation 14, and suppose $f_\Theta(x;\gamma,d) = w_\Theta(d)^\top x + \frac{\gamma}{2}\|x\|_2^2$ for any neural network $w_\Theta(d)$. For any $\alpha \in (0, 2/\gamma)$ define the sequence $\{z^k\}$ by:*

$$z^{k+1} = T_\Theta(z^k) \quad \text{for all } k \in \mathbb{N} \tag{29}$$

where

$$T_\Theta(z) \triangleq z - P_{\mathcal{C}_2}(z) + P_{\mathcal{C}_1}\left((2-\alpha\gamma)\, P_{\mathcal{C}_2}(z) - z - \alpha w_\Theta(d)\right). \tag{30}$$

If $x^k \triangleq P_{\mathcal{C}_2}(z^k)$ then $\|x^{k+1} - x^k\|_2^2 = O(1/k)$.

Proof. First note that $\nabla_x f_\Theta(x_\Theta;\gamma,d) = w_\Theta(d) + \gamma x$. Because $f_\Theta(x_\Theta;\gamma,d)$ is strongly convex, x_Θ is unique and is characterized by the first order optimality condition:

$$\nabla_x f_\Theta(x_\Theta;d)^\top (x - x_\Theta) \geq 0 \quad \text{for all } x \in \mathcal{C}. \tag{31}$$

Note that equation 31 can equally be viewed as a variational inequality with operator $F_\Theta(x;d) = \nabla_x f_\Theta(x_\Theta;d)$. We deduce that z_Θ with $x_\Theta = P_{\mathcal{C}_2}(z_\Theta)$ is a fixed point of

$$\begin{aligned} T_\Theta(z) &\triangleq z - P_{\mathcal{C}_2}(z) + P_{\mathcal{C}_1}\left(2 \cdot P_{\mathcal{C}_2}(z) - z - \alpha\left[w_\Theta(d) + \gamma P_{\mathcal{C}_2}(z)\right]\right) \\ &= z - P_{\mathcal{C}_2}(z) + P_{\mathcal{C}_1}\left((2-\alpha\gamma) \cdot P_{\mathcal{C}_2}(z) - z - \alpha w_\Theta(d)\right) \end{aligned} \tag{32a}$$

from McKenzie et al. (2021, Theorem 4.2), which is itself a standard application of ideas from operator splitting (Davis & Yin, 2017; Ryu & Yin, 2022).
As $\nabla_x f_\Theta(x_\Theta;\gamma,d)$ is γ-Lipschitz continuous it is also $\nabla_x f_\Theta$ is $1/\gamma$-cocoercive by the Baillon-Haddad theorem (Baillon & Haddad, 1977; Bauschke & Combettes, 2009). McKenzie et al. (2021, Theorem 3.3) then implies that $z^k \to z_\Theta$ but does not give a convergence rate. In fact, the convergence rate can be deduced from known results; because T_Θ is averaged for $\alpha < 2/\gamma$ the rate follows from Ryu & Yin (2022, Theorem 1). □

Next, we state two auxiliary lemmas relating the Jacobian matrices to projections onto linear subspaces.

Lemma 8. *If $\mathcal{C}_1 \triangleq \{x : Ax = b\}$, for full-rank $A \in \mathbb{R}^{m\times n}$, $b \in \mathbb{R}^n$ with $m < n$, and $\mathcal{H}_1 \triangleq \mathrm{Null}(A)$ then*

$$\frac{\partial P_{\mathcal{C}_1}}{\partial z} = P_{\mathcal{H}_1}, \quad \text{for all } z \in \mathbb{R}^n. \tag{33}$$

Proof. Let $A = U\Sigma V^\top$ denote the reduced SVD of A, and note that as $A \in \mathbb{R}^{m\times n}$ with $m < n$ we have $U \in \mathbb{R}^{m\times m}, \Sigma \in \mathbb{R}^{m\times m}$ and $V \in \mathbb{R}^{n\times m}$. Differentiating the formula for $P_{\mathcal{C}_1}$ given in Lemma 1 yields

$$\frac{\partial P_{\mathcal{C}_1}}{\partial z} = I - A^\dagger A, \tag{34}$$

where $A^\dagger \triangleq V\Sigma^{-1}U^\top$. Note

$$A^\dagger A = \left(V\Sigma^{-1}U^\top\right)\left(U\Sigma V^\top\right) = VV^\top, \tag{35}$$

which is the orthogonal projection onto $\mathrm{Range}(V) = \mathrm{Range}(A^\top)$. It follows that $I - A^\dagger A$ is the orthogonal projection on to $\mathrm{Range}(A^\top)^\perp = \mathrm{Null}(A)$. □

Lemma 9. *Define the multi-valued function*

$$c(\alpha) \triangleq \partial \max(0,\alpha) = \begin{cases} 1 & \text{if } \alpha > 0 \\ 0 & \text{if } \alpha < 0 \\ [0,1] & \text{if } \alpha = 0 \end{cases} \tag{36}$$

and, for $z \in \mathbb{R}^n$*, define* $\mathcal{H}_{2,z} \triangleq \text{Span}(e_i : z_i > 0)$*. Then*

$$\partial P_{\mathcal{C}_2}(\overline{z}) = \left[\frac{\mathrm{d}}{\mathrm{d}z}\,\text{ReLU}(z)\right]_{z=\overline{z}} = \text{diag}(c(\overline{z})), \tag{37}$$

and adopting the convention for choosing an element of $\partial P_{\mathcal{C}_2}(\overline{z})$ *stated in the main text:*

$$\left.\frac{\mathrm{d}P_{\mathcal{C}_2}}{\mathrm{d}z}\right|_{z=\overline{z}} = \text{diag}(\tilde{c}(\overline{z})) = P_{\mathcal{H}_{2,\overline{z}}}. \tag{38}$$

Proof. First, suppose $\overline{z} \in \mathbb{R}^n$ satisfies $\overline{z}_i \neq 0$, for all $i \in [n]$, *i.e.* $\overline{z}$ is a smooth point of $P_{\mathcal{C}_2}$. Note

$$\frac{\mathrm{d}[\text{ReLU}(\overline{z}_i)]}{\mathrm{d}z} = 1 \text{ if } i = j \text{ and } z_i > 0 \qquad \text{and} \qquad \frac{\mathrm{d}[\text{ReLU}(\overline{z}_i)]}{\mathrm{d}z} = 0 \text{ if } i \neq j \text{ or } z_i < 0. \tag{39}$$

Thus, the Jacobian matrix is diagonal with a 1 in the (i,i)-th position whenever $\overline{z}_i > 0$ and 0 otherwise, *i.e.* $\left.\frac{\mathrm{d}P_{\mathcal{C}_2}}{\mathrm{d}z}\right|_{z=\overline{z}} = \text{diag}(c(\overline{z}))$. Now suppose $z_i = 0$ for one i. For all $z \in \mathbb{R}^n$ with $z_i < 0$, the Jacobian $\left.\frac{\mathrm{d}P_{\mathcal{C}_2}}{\mathrm{d}z}\right|_{z}$ is well-defined and has a 0 in the (i,i)-th position, while for $z \in \mathbb{R}^n$ with $z_i > 0$, the Jacobian $\left.\frac{\mathrm{d}P_{\mathcal{C}_2}}{\mathrm{d}z}\right|_{z}$ is well-defined and has a 1 in the (i,i)-th position. Taking the convex hull yields the interval $[0,1]$ in the (i,i)-th position, as claimed. The case where $\overline{z}_i = 0$ for multiple i is similar.

Consequently, the product of $\left.\frac{\mathrm{d}P_{\mathcal{C}_2}}{\mathrm{d}z}\right|_{z=\overline{z}}$ and any vector $v \in \mathbb{R}^n$ equals v if and only if $v \in \text{Span}(e_i : \overline{z}_i > 0)$. This shows the linear operator is idempotent with fixed point set $\mathcal{H}_{2,\overline{z}}$, *i.e.* it is the projection operator $P_{\mathcal{H}_{2,\overline{z}}}$. □

Theorem 4. *Suppose* A *is full-rank and* $\mathcal{H}_1 \triangleq \text{Null}(A)$*,* $\mathcal{H}_{2,z} \triangleq \text{Span}\,(e_i : z_i > 0)$*. Then for all* $\hat{z} \in \mathbb{R}^n$

$$\left.\frac{\partial T_\Theta}{\partial z}\right|_{z=\overline{z}} = P_{\mathcal{H}_1^\perp} P_{\mathcal{H}_{2,\overline{z}}^\perp} + (1-\alpha\gamma)\cdot P_{\mathcal{H}_1} P_{\mathcal{H}_{2,\overline{z}}}. \tag{40}$$

Proof. Differentiating the expression for T_Θ in equation 30 with respect to z yields

$$\left.\frac{\partial T_\Theta}{\partial z}\right|_{z=\hat{z}} = I - \left.\frac{\mathrm{d}P_{\mathcal{C}_2}}{\mathrm{d}z}\right|_{z=\hat{z}} + \left.\frac{\mathrm{d}P_{\mathcal{C}_1}}{\mathrm{d}z}\right|_{z=y(\hat{z})} \left[(2-\alpha\gamma)\cdot \left.\frac{\mathrm{d}P_{\mathcal{C}_2}}{\mathrm{d}z}\right|_{z=\hat{z}} - I\right] \tag{41a}$$

$$= I - P_{\mathcal{H}_{2,\hat{z}}} + P_{\mathcal{H}_1}\left((2-\alpha\gamma)P_{\mathcal{H}_{2,\hat{z}}} - I\right), \quad \text{for all } \hat{z} \in \mathbb{R}^n, \tag{41b}$$

where, for notational brevity, we set $y(\hat{z}) \triangleq (2-\alpha\gamma)\cdot P_{\mathcal{C}_2}(\hat{z}) - \hat{z} - \alpha w_\Theta(d)$ in the first line and the second line follows from Lemmas 8 and 9. Repeatedly using the fact, for any subspace $\mathcal{H} \subset \mathbb{R}^n$, $P_{\mathcal{H}^\perp} = I - P_{\mathcal{H}}$, the derivative $\partial T_\Theta / \partial z$ can be further rewritten:

$$\left.\frac{\partial T_\Theta}{\partial z}\right|_{z=\hat{z}} = I - P_{\mathcal{H}_{2,\hat{z}}} + (2-\alpha\gamma)\cdot P_{\mathcal{H}_1} P_{\mathcal{H}_{2,\hat{z}}} - P_{\mathcal{H}_1} \tag{42a}$$

$$= P_{\mathcal{H}_{2,\hat{z}}^\perp} + (2-\alpha\gamma)\cdot P_{\mathcal{H}_1}\left(I - P_{\mathcal{H}_{2,\hat{z}}^\perp}\right) - P_{\mathcal{H}_1} \tag{42b}$$

$$= P_{\mathcal{H}_{2,\hat{z}}^\perp} + P_{\mathcal{H}_1} + (1-\alpha\gamma)\cdot P_{\mathcal{H}_1} - P_{\mathcal{H}_1} P_{\mathcal{H}_{2,\hat{z}}^\perp} - (1-\alpha\gamma)\cdot P_{\mathcal{H}_1} P_{\mathcal{H}_{2,\hat{z}}^\perp} - P_{\mathcal{H}_1} \tag{42c}$$

$$= (I - P_{\mathcal{H}_1}) P_{\mathcal{H}_{2,\hat{z}}^\top} + (1-\alpha\gamma)\cdot P_{\mathcal{H}_1}(I - P_{\mathcal{H}_{2,\hat{z}}^\perp}) \tag{42d}$$

$$= P_{\mathcal{H}_1^\perp} P_{\mathcal{H}_{2,\hat{z}}^\perp} + (1-\alpha\gamma)\cdot P_{\mathcal{H}_1} P_{\mathcal{H}_{2,\hat{z}}}, \quad \text{for all } \hat{z} \in \mathbb{R}^n, \tag{42e}$$

completing the proof. □

We use the following lemma to prove Theorem 6.

Lemma 10. *If the LICQ condition holds at* x_Θ*, then* $\mathcal{H}_1^\perp \cap \mathcal{H}_{2,z_\Theta}^\perp = \{0\}$*.*

Proof. We first rewrite $\mathcal{H}_1^\perp$ and $\mathcal{H}_{2,z_\Theta}^\perp$. The subspace $\mathcal{H}_{2,z_\Theta}^\perp$ is spanned by all non-positive coordinates of z_Θ. By equation 17, $[x_\Theta]_i = \max\{0, [z_\Theta]_i\}$, and so $i \in \mathcal{A}(x_\Theta)$ if and only if $[z_\Theta]_i \leq 0$. It follows that

$$\mathcal{H}_{2,z_\Theta}^\perp \triangleq \text{Span}\{e_i : [z_\Theta]_i \leq 0\} = \text{Span}\{e_i : i \in \mathcal{A}(x_\Theta)\} = \text{Span}\{e_{i_1}, \dots, e_{i_\ell}\}, \tag{43}$$

where we enumerate $\mathcal{A}(x_\Theta)$ via $\mathcal{A}(x_\Theta) = \{i_1, \dots, i_\ell\}$. On the other hand, $\mathcal{H}_1^\perp = \text{Range}(A^\top) = \text{Span}(a_1, \dots, a_m)$ where $a_i^\top$ denotes the i-th row of A.

Let $v \in \mathcal{H}_1^\perp \cap \mathcal{H}_{2,z_\Theta}^\perp$ be given. Since $v \in \mathcal{H}_1^\perp$, there are scalars $\alpha_1, \dots, \alpha_\ell$ such that $v = \alpha_1 e_{i_1} + \dots + \alpha_\ell e_{i_\ell}$. Similarly, since $v \in \mathcal{H}_{2,z_\Theta}^\perp$, there are scalars $\beta_1, \dots, \beta_m$ such that $v = \beta_1 a_1 + \dots + \beta_m a_m$. Hence

$$0 = v - v = \big(\alpha_1 e_{i_1} + \ldots + \alpha_\ell e_{i_\ell}\big) - \big(\beta_1 a_1 + \ldots + \beta_m a_m\big). \tag{44}$$

By the LICQ condition, $\{e_{i_1}, \dots, e_{i_\ell}\} \cup \{a_1, \dots, a_m\}$ is a linearly independent set of vectors; hence $\alpha_1 = \ldots = \alpha_\ell = \beta_1 = \ldots = \beta_m = 0$ and, thus, $v = 0$. Since v was arbitrarily chosen in $\mathcal{H}_1^\perp \cap \mathcal{H}_{2,z_\Theta}^\perp$, the result follows. ☐

Theorem 6. *If the LICQ condition holds at x_Θ, A is full-rank and $\alpha \in (0, 2/\gamma)$, then $\|\partial T_\Theta / \partial z\|_{z=z_\Theta} < 1$.*

Proof. By Lemma 10, the LICQ condition implies $\mathcal{H}_1^\perp \cap \mathcal{H}_{2,z_\Theta}^\perp = \{0\}$. This implies that either (i) the first principal angle τ between these two subspaces is nonzero, and so the cosine of this angle is less than unity, *i.e.*

$$1 > \cos(\tau) \triangleq \max_{u \in \mathcal{H}_1^\perp : \|u\|=1} \max_{v \in \mathcal{H}_{2,z}^\perp : \|v\|=1} \langle u, v \rangle, \tag{45}$$

or (ii) (at least) one of $\mathcal{H}_1^\perp, \mathcal{H}_{2,z_\Theta}^\perp$ is the trivial vector space $\{0\}$. In either case, let $w \in \mathbb{R}^n$ be given. By Theorem 4, in case (ii)

$$\left[\frac{\partial T_\Theta}{\partial z} w\right]_{z=z_\Theta} = P_{\mathcal{H}_1^\perp} P_{\mathcal{H}_{2,z_\Theta}^\perp} w + (1 - \alpha\gamma) \cdot P_{\mathcal{H}_1} P_{\mathcal{H}_{2,z_\Theta}} w = (1 - \alpha\gamma) \cdot P_{\mathcal{H}_1} P_{\mathcal{H}_{2,z_\Theta}} w \tag{46}$$

implying that

$$\left\|\frac{\partial T_\Theta}{\partial z} w\right\|_{z=z_\Theta} = (1 - \alpha\gamma) \left\|P_{\mathcal{H}_1} P_{\mathcal{H}_{2,z_\Theta}} w\right\| \leq (1 - \alpha\gamma)\|w\|, \tag{47}$$

where the inequality follows as projection operators are firmly nonexpansive. In case (i), write $w = w_1 + w_2$, where $w_1 \in \mathcal{H}_{2,z_\Theta}$ and $w_2 \in \mathcal{H}_{2,z_\Theta}^\perp$. Appealing to Theorem 4 again

$$\left[\frac{\partial T_\Theta}{\partial z} w\right]_{z=z_\Theta} = P_{\mathcal{H}_1^\perp} P_{\mathcal{H}_{2,z_\Theta}^\perp} w + (1 - \alpha\gamma) \cdot P_{\mathcal{H}_1} P_{\mathcal{H}_{2,z_\Theta}} w = P_{\mathcal{H}_1^\perp} w_2 + (1 - \alpha\gamma) \cdot P_{\mathcal{H}_1} w_1. \tag{48}$$

Pythagoras' theorem may be applied to deduce, together with the fact $P_{\mathcal{H}_1^\perp} w_2$ and $P_{\mathcal{H}_1} w_1$ are orthogonal,

$$\left\|\frac{\partial T_\Theta}{\partial z} w\right\|_{z=z_\Theta}^2 = \left\|P_{\mathcal{H}_1^\perp} w_2\right\|^2 + (1 - \alpha\gamma)^2 \cdot \|P_{\mathcal{H}_1} w_1\|^2. \tag{49}$$

Since $w_2 \in \mathcal{H}_{2,z_\Theta}^\perp$, the angle condition (45) implies

$$\left\|P_{\mathcal{H}_1^\perp} w_2\right\|^2 = \langle P_{\mathcal{H}_1^\perp} w_2, P_{\mathcal{H}_1^\perp} w_2 \rangle = \langle w_2, P_{\mathcal{H}_1^\perp} P_{\mathcal{H}_1^\perp} w_2 \rangle = \langle w_2, P_{\mathcal{H}_1^\perp} w_2 \rangle \leq \cos(\tau) \cdot \|w_2\|^2, \tag{50}$$

where the third equality holds since orthogonal linear projections are symmetric and idempotent. Because projections are non-expansive and $P_{\mathcal{H}_{2,z_\Theta}}$ is linear,

$$\|P_{\mathcal{H}_1} w_1\|^2 = \|P_{\mathcal{H}_1} w_1 - P_{\mathcal{H}_1} 0\|^2 \leq \|w_1 - 0\|^2 = \|w_1\|^2. \tag{51}$$

Combining (49), (50) and (51) reveals

$$\begin{aligned}\left\|\frac{\partial T_\Theta}{\partial z} w\right\|^2_{z=z_\Theta} &\leq \cos(\tau)\cdot\|w_2\|^2 + (1-\alpha\gamma)^2\|w_1\|^2 && \text{(52a)}\\ &\leq \max\{\cos(\tau),(1-\alpha\gamma)^2\}\cdot\left(\|w_1\|^2+\|w_2\|^2\right) && \text{(52b)}\\ &= \max\{\cos(\tau),(1-\alpha\gamma)^2\}\cdot\|w\|^2, && \text{(52c)}\end{aligned}$$

noting the final equality holds since w_1 and w_2 are orthogonal. Because (52) holds for arbitrarily chosen $w \in \mathbb{R}^n$,

$$\left\|\frac{\partial T_\Theta}{\partial z}\right\|_{z=z_\Theta} \triangleq \sup\left\{\left\|\frac{\partial T_\Theta}{\partial z} w\right\|_{z=z_\Theta} : \|w\| = 1\right\} \leq \sqrt{\max\{\cos(\tau),(1-\alpha\gamma)^2\}} < 1, \tag{53}$$

where the final inequality holds by (45) and the fact $\alpha \in (0, 2/\gamma)$ implies $1-\alpha\gamma \in (-1,1)$, as desired. ☐

Corollary 7. *If T_Θ is continuously differentiable with respect to Θ at z_Θ, the assumptions in Theorem 6 hold and $(\partial T_\Theta/\partial\Theta)^\top(\partial T_\Theta/\partial\Theta)$ has condition number sufficiently small, then $p_\Theta(x_\Theta)$ is a descent direction for ℓ with respect to Θ.*

Proof. From the proof of Theorem 6 we see that T_Θ is contractive with constant $\Gamma = \sqrt{\max\{\cos(\tau),(1-\alpha\gamma)^2\}}$ and so the main theorem of (Fung et al., 2022), guaranteeing p_Θ is a descent direction, as long as the condition number of $(\partial T_\Theta/\partial\Theta)^\top(\partial T_\Theta/\partial\Theta)$ is less than $1/\Gamma$. ☐

Remark 11. *Similar guarantees, albeit with less restrictive assumptions on $\partial T_\Theta/\partial\Theta$, can be deduced from the results of the recent work (Bolte et al., 2024).*

B Derivation for Canonical Form of Knapsack Prediction Problem

For completeness, we explain how to transform the k-knapsack prediction problem into the canonical form equation 8, and how to derive the standardized representation of the constraint polytope $\mathcal{C}$. Recall that the k-knapsack prediction problem, as originally stated, is

$$x^\star = \operatorname*{arg\,max}_{x\in\mathcal{X}} w^\top x \text{ where } \mathcal{X} = \{x \in \{0,1\}^\ell : \ Sx \leq c\} \text{ and } S = \begin{bmatrix} s_1 & \cdots & s_\ell\end{bmatrix} \in \mathbb{R}^{k\times\ell} \tag{54}$$

We introduce slack variables $y_1,\ldots,y_k$ so that the inequality constraint $Sx \leq c$ becomes

$$\begin{aligned} -Sx + c \geq 0 &\Longrightarrow -Sx + c = y \text{ and } y \geq 0\\ &\Longrightarrow \begin{bmatrix} S & I_k\end{bmatrix}\begin{bmatrix} x\\ y\end{bmatrix} = c\end{aligned}$$

We relax the binary constraint $x_i \in \{0,1\}$ to $0 \leq x_i \leq 1$. We add additional slack variables $z_1,\ldots,z_\ell$ to account for the upper bound:

$$1 - x_i \geq 0 \Longrightarrow 1 - x_i = z_i \text{ and } z_i \geq 0 \Longrightarrow \begin{bmatrix} I_{\ell\times\ell} & 0_{\ell\times k} & I_{\ell\times\ell}\end{bmatrix}\begin{bmatrix} x\\ y\\ z\end{bmatrix} = \mathbf{1} \tag{55}$$

Putting this together, define

$$A = \begin{bmatrix} -S & -I_{k\times k} & 0_{k\times\ell}\\ I_{\ell\times\ell} & 0_{\ell\times k} & I_{\ell\times\ell}\end{bmatrix} \in \mathbb{R}^{(k+\ell)\times(2\ell+k)} \text{ and } b = \begin{bmatrix} -c\\ \mathbf{1}_\ell\end{bmatrix} \in \mathbb{R}^{k+\ell} \tag{56}$$

Finally, redefine $x = \begin{bmatrix} x & y & z\end{bmatrix}^\top$ and $w = \begin{bmatrix} -w & \mathbf{0}_k & \mathbf{0}_\ell\end{bmatrix}$ (where we're using $-w$ to switch the argmax to an argmin) and obtain:

$$x^\star = \operatorname*{arg\,min}_{x\in\mathrm{Conv}(\mathcal{X})} w^\top(d)x + \gamma\|x\|_2^2 \text{ where } \mathrm{Conv}(\mathcal{X}) = \{x : Ax = b \text{ and } x \geq 0\} \tag{57}$$

C Experimental Details

C.1 Additional Data Details for Knapsack Problem

As mentioned, we use PyEPO (Tang & Khalil, 2022) to generate the training data. Specifically, $d \in \mathbb{R}^5$ is sampled from the multivariate Gaussian distribution with mean 0 and covariance I. Then, $B \in \mathbb{R}^{n \times 5}$ is sampled where each $B_{ij} = +1$ with probability 0.5 and -1 with probability 0.5. The associated cost vector $w(d)$ is computed as

$$[w(d)]_i = \left[\frac{1}{3.5^{\text{deg}}} \left(\frac{1}{\sqrt{5}} (Bd)_i + 3 \right)^{\text{deg}} + 1 \right] \cdot \epsilon_{ij}$$

where deg $= 4$ and ϵ_{ij} is sampled uniformly from the interval $[0.5, 1.5]$.

C.2 Additional Training Details for Knapsack Problem

For all models we use an initial learning rate of 10^{-3} and a scheduler that reduces the learning rate whenever the validation loss plateaus. We also used weight decay with a parameter of 5×10^{-4}. All networks were trained using a AMD Threadripper Pro 3955WX: 16 cores, 3.90 GHz, 64 MB cache, PCIe 4.0 CPU and an NVIDIA RTX A6000 GPU.

C.3 Additional Model Details for Large-Scale Shortest Path Problem

Our implementation of `PertOpt-net` used a PyTorch implementation[7] of the original TensorFlow code[8] associated to the paper Berthet et al. (2020). We experimented with various hyperparameter settings for 5-by-5 grids and found setting the number of samples equal to 3, the temperature (*i.e.* ε) to 1 and using Gumbel noise to work best, so we used these values for all other shortest path experiments. Our implementation of `BB-net` uses the `blackbox-backprop` package[9] associated to the paper Pogančić et al. (2019). We found setting $\lambda = 5$ (see Pogančić et al. (2019) for a description of this hyperparameter) to work best for 5-by-5 grids, so we use this value for all other shortest path experiments.

C.4 Additional Training Details for Shortest Path

We use the MSE loss to train `DYS-net`, `PertOpt-net`, and `CVX-net`. We tried using the MSE loss with `BB-net` but this did not work well, so we used the Hamming (also known as 0–1) loss, as done in Pogančić et al. (2019).

To train `DYS-net` and `CVX-net`, we use an initial learning rate of 10^{-2} and use a scheduler that reduces the learning rate whenever the test loss plateaus—we found this to perform the best for these two models. For `PertOpt-net` we found that using a fixed learning rate of 10^{-2} performed the best. For `BB-net`, we performed a logarithmic grid-search on the learning rate between $10{-}1$ to 10^{-4} and found that 10^{-3} performed best; we also attempted adaptive learning rate schemes such as reducing learning rates on plateau but did not obtain improved performance.

All networks were trained using a AMD Threadripper Pro 3955WX: 16 cores, 3.90 GHz, 64 MB cache, PCIe 4.0 CPU and an NVIDIA RTX A6000 GPU.

D Additional Experimental Results

In Figure 6, we show the test loss and training time per epoch for all three architectures: `DYS-net`, `CVX-net`, and `PertOpt-net` for 10-by-10, 20-by-20, and 30-by-30 grids. In terms of MSE loss, `CVX-net` and `DYS-net` lead to comparable performance. In the second row of Figure 6, we observe the benefits of combining the three-operator splitting with JFB (Fung et al., 2022); in particular, `DYS-net` trains much faster. Figure 7 shows some randomly selected outputs for the three architectures once fully trained.

[7]See code at `github.com/tuero/perturbations-differential-pytorch`

[8]See code at `github.com/google-research/google-research/tree/master/perturbations`

[9]See code at `https://github.com/martius-lab/blackbox-backprop`

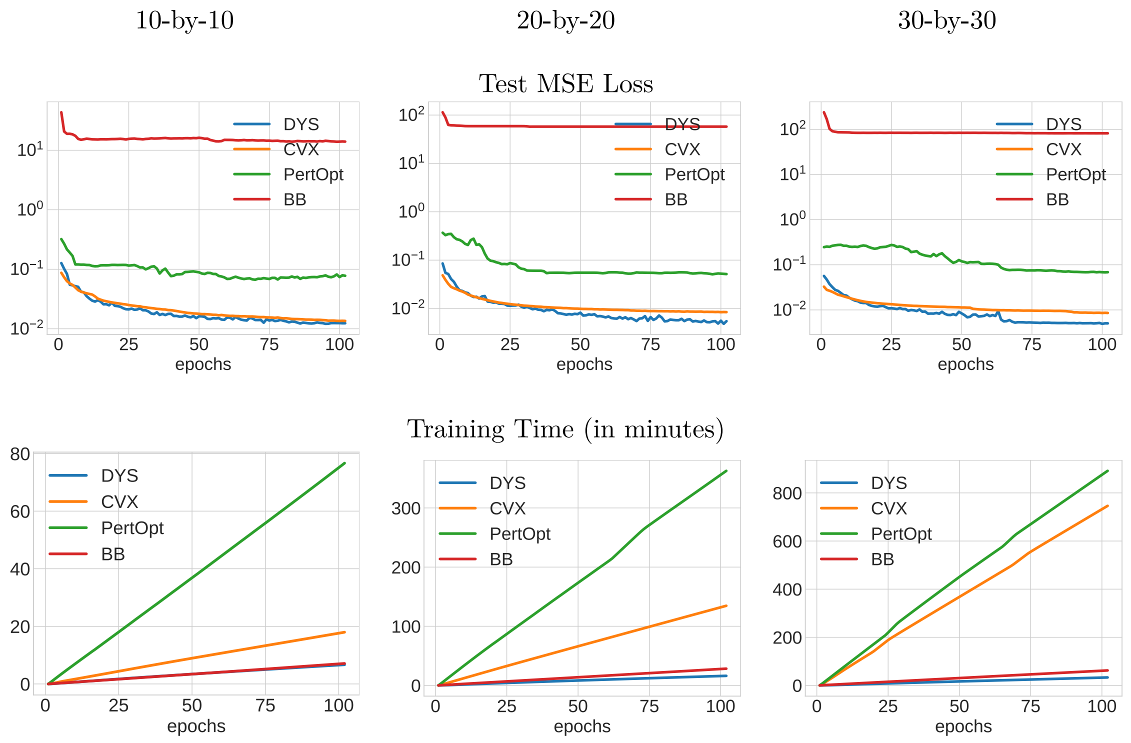

Figure 6: Comparison of of DYS-Net, `cvxpylayers` (Agrawal et al., 2019a), PertOptNet (Berthet et al., 2020), and Blackbox Backpropagation-net (BB-Net) (Pogančić et al., 2019) for three different grid sizes: 10×10 (first column), 20×20 (second column), and 30×30 (third column). The first row shows the MSE loss vs. epochs of the testing dataset. The second row shows the training time vs. epochs.

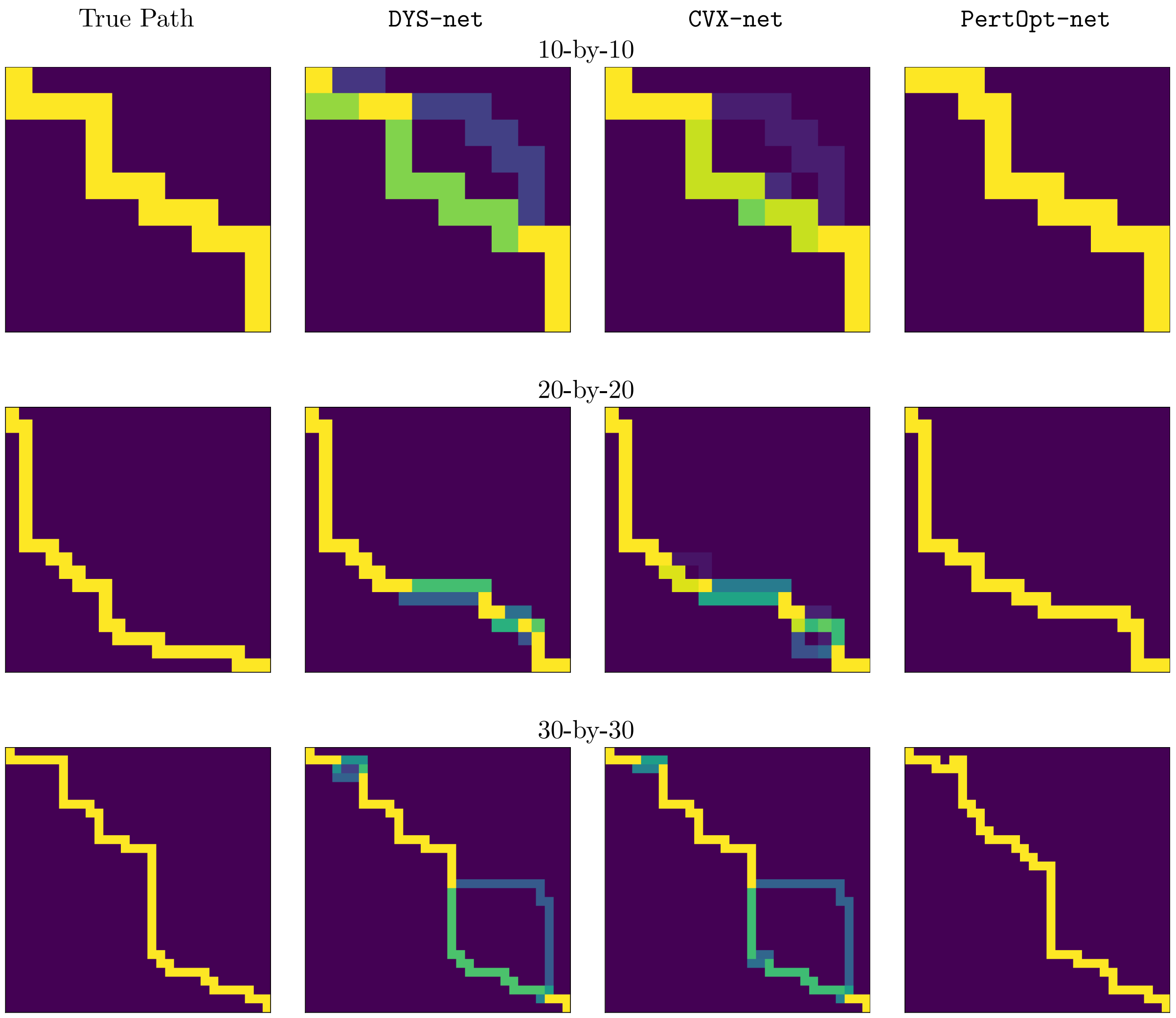

Figure 7: True paths (column 1), paths predicted by **DYS-net** (column 2), **CVX-net** (column 3), and **PertOpt-net** (column 4). Samples are taken from different grid sizes: 10-by-10 (row 1), 20-by-20 (row 2), and 30-by-30 (row 3).